Japan Geoscience Union Meeting 2015
(May 24th - 28th at Makuhari, Chiba, Japan)

SSS30-01 Room:A05 Time:May 25 09:00-09:15

Shear stress distributions of a subduction zone as inferred from elastic plate models

YOSHIDA, Mitsuru[1*]

[1]none

It is important to understand shear stress and fracture strength of a sesismogenic zone for the study of a seismogenesis mechanism. Shear stress characterisics of elastic oceanic and continental plates near a subduction zone are investigated using 2D finte element method in the case of plane strain. The present elastic plate model UMB-Plate (Figure) is composed of oceamic plate (Plate 1), continental plate (Plate 2), upper mantle (LMS), and two transitional layers, a plate boundary (PB) layer between Plate 1 and Plate 2 and an upper mantle boundary (UMB) layer between LMS and Plate 1. The two transitional layers correspond to low viscosity layers.

The Young's modulai (E) and Poisson's ratios (p) for Plate 1, Plate 2, and LMS are adopted from those used in the study of earthquake cycle simulation in Southwest Japan (Hori, et al., 2004). The Young's modulus is calculated from the rigidity (G) using the formula E=2(1+p)G (Tokawa, 1980). Young's modulus of mild steel of rubber-like-elasticity (Rikagakuziten, 1988) and Poisson's ratio of elastic rubber (Rika nenpyo, 2002) are used for those of PB and UMB. The size of the model is 625 and 325 mm in x- and y-directions, respectively, the thickness being 2 mm. The lengths enlarged to 200,000 times are ahown in the figure. A horizontal compressive force of 1.4 ton corresponding to a ridge push force of 4.7 MPa is applied to the left side of Plate 1. The right side of Plate 2 is fixed. The right side of Plate 1 is firstly assumed to be stress free. The dip angle of the subducting oceanic plate (Plate 1) is 10 deg. at shallow parts between sites C and I and 27 dig. at deeper parts between sites I and X. Site I corresponds to a convergent boundary.

The shear stresses calculated for UMB-Plate show that they are positive as a whole for Plate 2 above PB and are mostly negative for Plate 1. A positive shear stress zone exists in the inner part of Plate 1 at depths of 10-30 km beneath site C. The region showing a maximum shear stress of 1.095 MPa is located at edge of Plate 2 near site I. High shear stress zones are distributed at the thrust zone in Plate 2 above PB at depths less than 30 km. The region showing a minimum shear stress of -2.8x10E-06 MPa is located at a lower part of UMB near at a depth of 55 km. Mises stress defined by shear strain energy, which is one of the yield criterion (Kikuchi and Wada, 2004), is also highest at the left side of Plate 2 beneath site I, with a maximum stress of 19.25 MPa.

The elastic model UMB-Plate does not specify any particular region in Japanese island arc. However, the thickness 30 km and length 60 km of the oceanic plate is rather close to the vertical section of the crust and upper mantle in the Tokai district, Southwest Japan. If the slab is short the earthquake mechanism in the slab is likely to show a normal fault in the negative shear stress field and the thrust zone is characterized by a low-angle reverse fault in the positive shear stress field (Seno. 2001). The shear stress distributions calculated seem to be in harmony with the stress field mentioned above.

The effects of negative buoyancy which corresponds to a slab pull force were examined. If the downward pull force is applied to the right side of Plate 1, the area showing a positive shear stress increases inside the subducting Plate 1, while the area showing a negative shear stress increases inside Plate 2.

Figure. Configulation of elastic plate model UMB-Plate and elastic constants of media.

Keywords: Shear stress, Subduction zone, Elastic plate model, 2D FEM

Keywords: shear stress, subducion zone, elastic plate model, 2D FEM

SSS30-01 Room:A05 Time:May 25 09:00-09:15

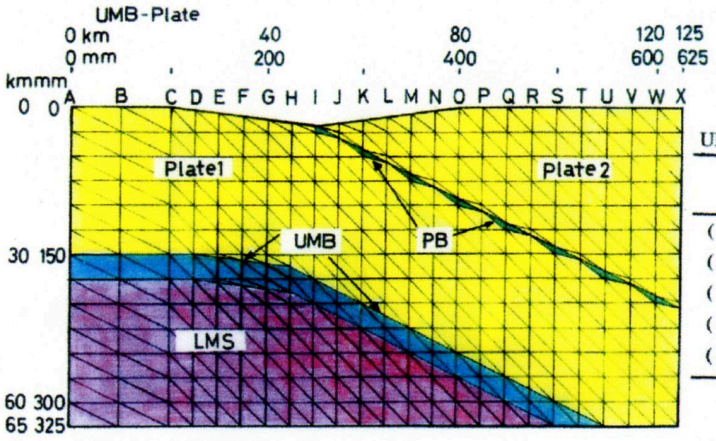

UMB-Plate

No.	Young's Modulus [MPa]	Poisson's ratio
(1) Plate 1	$1.65 * 10^5$	0.25
(2) Plate 2	$1.65 * 10^5$	0.25
(3) PB	1.65	0.46
(4) UMB	1.65	0.46
(5) LMS	$1.708 * 10^5$	0.298

Japan Geoscience Union Meeting 2015
(May 24th - 28th at Makuhari, Chiba, Japan)

SSS30-02 Room:A05 Time:May 25 09:15-09:30

Two-dimensional fully dynamic spectral-element simulations of long-term in-plane shear fault slip

SHIMIZU, Hiroyuki[1] ; KANEKO, Yoshihiro[2] ; HIRAHARA, Kazuro[1*]

[1]Graduate School of Science, Kyoto University, [2]GNS Science

Earthquake cycle simulations have been performed to successfully reproduce historical earthquake occurrences (eg. Tse and Rice 1986; Stuart, 1988). Most of them are based on a quasi-dynamic scheme, where inertial effects are approximated by the radiation damping term proposed by Rice (1993). This is because a “fully-dynamic” scheme that accounts for all the inertial effects requires quite large CPU and memory cost. Lapusta et al. (2000, 2009) developed a methodology capable of simulating seismic and aseismic slip and gradual process of earthquake nucleation over the entire earthquake cycle. Their fully-dynamic simulations have produced earthquake cycles considerably different from quasi-dynamic ones (Thomas et al., 2014). Those simulations have, however, never been performed for interplate earthquakes at subduction zones, because their models based on a spectral boundary integral method are currently limited to relatively simple fault geometry.

Many studies showed that, for rupture on a dipping fault such as interplate earthquakes at subduction zones, normal stress is altered during faulting due to the interaction with the Earth’s free surface. This change in normal stress not only affects the earthquake rupture process, but also causes the residual stress variation that might affect the long-term histories of earthquake cycles (Duan and Oglesby, 2005). Therefore it is important to account for both the dipping fault geometry and the dynamic effects.

Recently, Kaneko et al. (2011) have performed the fully dynamic spectral-element method (SEM) simulations of the long-term anti-plane fault slip. They combined quasi-static and fully-dynamic SEM schemes for simulating entire earthquake cycles. Aiming at simulating interplate earthquake cycles at subduction zones, we extend their study to simulations for in-plane shear faults and implement our numerical scheme in a dynamic rupture SEM code (Ampuero, 2002). Unlike the anti-plane cases, an in-plane shear fault requires modifications of the fault-perpendicular displacements, which were neglected in Kaneko et al. (2011). While this is implicitly calculated in BIEM (Boundary Integral Equation Method) simulations, we have to explicitly update such values in the domain method like SEM.

We perform fully-dynamic earthquake cycle simulations of long-term slip on a simple planar fault embedded in an elastic medium as described in Kaneko et al. (2011; Fig.2) except that we consider an in-plane fault and use quasi-dynamic updating scheme during the interseismic periods. The central portion of the fault is governed by the rate-and-state friction and both sides of the fault are steady-sliding velocity boundaries. Our numerical code is verified by the convergence of the results with several different discretization sizes, and by approximately the same recurrence times for the cases of anti-plane and in-plane faults, where the same nucleation sizes are obtained by adjusting frictional parameters. The code also works well for a vertical fault in an elastic half space. We discuss the differences between the dynamic and quasi-dynamic simulations.

We also discuss applications of our updated SEM scheme to the dipping fault. For dipping fault rupture such as the 2011 Tohoku earthquake in a homogeneous elastic half-space, we successfully simulate scenarios of single dynamic rupture propagation. However, we have some problems in simulating quasi-static interseismic simulations at present for this case.

Keywords: computational seismology, earthquake cycle, rate and state friction law, spectral element method, fully dynamic, interplate earthquake

Japan Geoscience Union Meeting 2015
(May 24th - 28th at Makuhari, Chiba, Japan)

SSS30-03 Room:A05 Time:May 25 09:30-09:45

Forecast experiments using friction law on occurrence times of the Kamaishi repeating earthquakes

YOSHIDA, Shingo[1*] ; KATO, Naoyuki[1] ; FUKUDA, Jun'ichi[1]

[1]ERI, Univ. Tokyo

Uchida et al. (2014) reported that a repeating earthquake sequence on the plate boundary off the shore of Kamaishi showed a regular recurrence interval before the 2011 Tohoku-oki earthquake (M9). After the Tohoku-oki earthquake, the repeaters showed increases in magnitude and shorter recurrence intervals. A M6 class event occurred just after the M9 event. Uchida et al. (2014) proposed a conceptual model in which conditionally stable regions and unstable regions are distributed. Using this model, Yoshida, Kato, and Fukuda (2015) conducted numerical simulations of the Kamaishi repeaters assuming the afterslip obtained by Fukuda et al (2013). In this simulation, a M6 class event was reproduced, and the calculated occurrence times of the following repeaters resembled the observation to some degree.

In this study, we perform trial experiments on occurrence time forecast of the Kamaishi repeaters. 11 events occurred after the M9 events. Assuming various parameters, we calculate the occurrence times of the 10 events before the latest event. We select proper models by evaluating these models, and calculate the occurrence time of the 11th event using the selected models. Average of the calculated times would provide an estimate. We discuss how we should evaluate the models, and incorporate simulations into prediction schemes.

Keywords: Kamaishi repeaters, occurrence time, prediction experiment, numerical simulation, rate and state dependent friction law, afterslip

Japan Geoscience Union Meeting 2015
(May 24th - 28th at Makuhari, Chiba, Japan)

SSS30-04 Room:A05 Time:May 25 09:45-10:00

Adequate Emplacement of the Data Assimilation Window and Sensitivity Analysis

HIYOSHI, Yoshihisa[1*] ; SUGIURA, Nozomi[1] ; HORI, Takane[1]

[1]JAMSTEC

Comprehension of fault behavior in earthquake sequence inevitably requires to elucidate frictional properties on slip interfaces. One of the good candidates to grasp the properties is data assimilation.

Recently Kano et al. (2013) developed a methodology for applying an adjoint-based data assimilation method to constrain some of the frictional properties on a simplified fault model with synthetic afterslip observation data. They found that all the frictional parameters were optimized when both acceleration and deceleration phases of the observed slip-rate data were assimilated. Importance of their finding is that an adequate emplacement of the assimilation time window plays one of the key roles to optimize the frictional parameters.

In this research, we attempt to find where the assimilation time window should be placed on to constrain all the frictional parameters. It could be acceptable that the assimilation time window should cover portions of the slip rate time series having the highest sensitivity to perturbations of the frictional properties. To ensure the above notion, we make theoretical and numerical approaches.

First, we set a simplified fault model with a rate- and state-dependent law and an aging law, sketching characteristics of the long-term slow slip events (SSEs) recurring on the plate interface beneath the Bungo Channel in southwest Japan.

For searching the portions of the highest sensitivity, we take a first variation of the governing equations of the SSE model. This algebraic manipulation shows that the highest sensitivity appears in the acceleration phase of the slip rate time series.

We then make a series of synthetic data assimilation experiments to examine whether or not the highest sensitivity portion offer an adequate assimilation window. The experiments employ an adjoint data assimilation method to constrain frictional parameters of the Bungo SSE model with synthetic slip rate observation data.

In our presentation, we will demonstrate the results of the experiments that the acceleration part of the slip rate is expected to be necessary to retrieve all the frictional parameters on the slip interfaces.

Combining the results of the mathematical formulation and the synthetic data assimilation experiments, we may confirm that an adequate assimilation time window spans the portions having the highest sensitivity to perturbations of the frictional parameters. Also, the distribution of the sensitivities in the slip rate time series could be obtained as a priori knowledge through the algebraic manipulation of the governing equations.

Keywords: data assimilation, sensitivity analysis, adjoint method

Japan Geoscience Union Meeting 2015
(May 24th - 28th at Makuhari, Chiba, Japan)

SSS30-05 Room:A05 Time:May 25 10:00-10:15

Power spectral density of slip distribution and slip rate function

HIRANO, Shiro[1*] ; YAGI, Yuji[2]

[1]University of Tsukuba, [2]University of Tsukuba

In view of energetics, earthquake faulting is a physical process that part of cumulated strain (i.e., potential) energy is converted into radiated (i.e., kinetic) energy. We have revealed that the potential energy and kinetic energy can be represented by quite similar spectral integrals although the former is with respect to spatial wavenumber and the latter is with respect to frequency[1]. In other words, power spectral densities (PSD) of the potential energy, which is correlated to slip distribution[2], and kinetic energy, which is correlated to slip rate function, are related to each other. This seems to be reasonable qualitatively because shorter wavelength components of the slip distribution should generate higher frequency contents of the seismic wave. To investigate this relationship quantitatively, we model spatio-temporal distribution of slip rate function on the fault and show that PSD of slip distribution and PSD of slip rate function should have the similar form. In our model, the distribution of slip rate function is represented as spatial distribution of peak slip velocity multiplied by a characteristic slip rate function that arises when the rupture front arrives at each point; this is an extension of the Haskell model. We find that the PSDs are proportional to a PSD of distribution of the peak slip velocity even if the distribution is quite heterogeneous and rupture velocity has perturbation in space. This suggests that the PSD of the slip distribution, which is hardly analyzed due to poor resolution of slip inversion analyses, can be roughly estimated by using the PSD of slip rate function of an ideal point source. Additionally, our model of the characterized slip rate function is consistent with a result of dynamic simulation of spontaneous rupture propagation along a rough fault[3]. Hence we suggest a simple method to estimate not only heterogeneity of slip distribution but also roughness of faults.

References

[1] Hirano, S., & Yagi, Y., 2014, Dependence of Seismic Energy on Higher Wavenumber Components, *AGU Fall Meeting*, S53B-4505.

[2] Mai, P.M., & Beroza, G.C., 2002, A Spatial Random Field Model to Characterize Complexity in Earthquake Slip, *J. Geophys. Res.*, **107**(B11) 2308.

[3] Trugman, D.T., & Dunham, E.M., 2014, A 2D Pseudodynamic Rupture Model Generator for Earthquakes on Geometrically Complex Faults, *Bull. Seism. Soc. Am.*, **104**(1) 95-112

Keywords: Slip inversion, Power spectral density, Earthquake energy budget, Heterogeneous fault

Japan Geoscience Union Meeting 2015
(May 24th - 28th at Makuhari, Chiba, Japan)

SSS30-06 Room:A05 Time:May 25 10:15-10:30

Fractal fault zone geometry and scale-dependent static stress drop

OTSUKI, Kenshiro[1*]

[1]Department of Geology, Graduate School of Science, Tohoku Univ.

I have shown that fault zone geometries, composed of fault segments and jog, are hierarchically selfsimilar (Fig.1a). This inhomogeneous structure breaks down the wellknown relations among fault length, averaged seismic slip and seismic moment. The distribution of seismic slip also is pinned hierarchically by jogs, showing a spectral distribution (Fig.1b). Based on the high quality data of fault traces and slip distributions from 21 surface earthquake strike-slip faults, here I show that average static stress drop $\triangle\sigma$ decreases as L_0.

Key Point 1
If $D_{av}$of a fault (L, D_{max}) is $\pi D_{max}/4$, $\triangle\sigma = C\pi D_{max}/4L$.
For a fault composed of linked n faults with (L/n, D_{max}) also $D_{av} = \pi D_{max}/4$, while $\triangle\sigma = nC\pi D_{max}/4L$.
[Symbol fault length:L, maximum slip:D_{max} and averaged slip:D_{av}, static stress drop:$\triangle\sigma$, proportional constant:C]

Key Point 2
Slip distributions D_x on fault segments are approximated by two simple cases below.
Cases of homogeneous frictional resistance $D_x = 2(1 - \nu)/G \times ({\sigma_{yx}}^r - {\sigma_{yx}}^c) \times (a^2 - x^2)^{0.5}$.
Cases of frictional resistance with a linear gradient $D_x = (1 - \nu)/G \times (2{\sigma_{yx}}^r - {\sigma_{yx}}^c(x/a)) \times (a^2 - x^2)^{0.5}$.
[Symbol half length of fault segments:a, Poisson's ratio:ν, remote stress:${\sigma_{xy}}^r$, frictional resistance:${\sigma_{xy}}^c$]

Key Point 3
When $L_s(i,j) < W_s$, $\triangle\sigma_{av}(i,j) = (7\pi G/8)(D_{av}(i,j)/L_s(i,j)$.
When $Ls(i,j) > W_s$, $\triangle\sigma_{av}(i,j) = (2G/\pi)(D_{av}(i,j)/W_s$.
The static stress drops averaged over the whole fault length L_0 is $\triangle\sigma = (\sum\triangle\sigma_{av}(i,j)L_s(i,j)/L_0$.
[Symbol for j-th segment of hierarchical rank i, segment length:$L_s(i,j)$, averaged slip:$D_{av}(i,j)$, static stress drop:$\triangle\sigma_{av}(i,j)$, thickness of seismogenic crustal layer:W_s, rigidity:G]

Analytical Results
17 among 21 data are approximated to the equation below (Fig.1c).
$\triangle\sigma = 79.0\ {L_0}^{-0.519}$ (units km and MPa)

Keywords: static stress drop, scale dependence, fault zone geometry, hierarchically selfsimilar

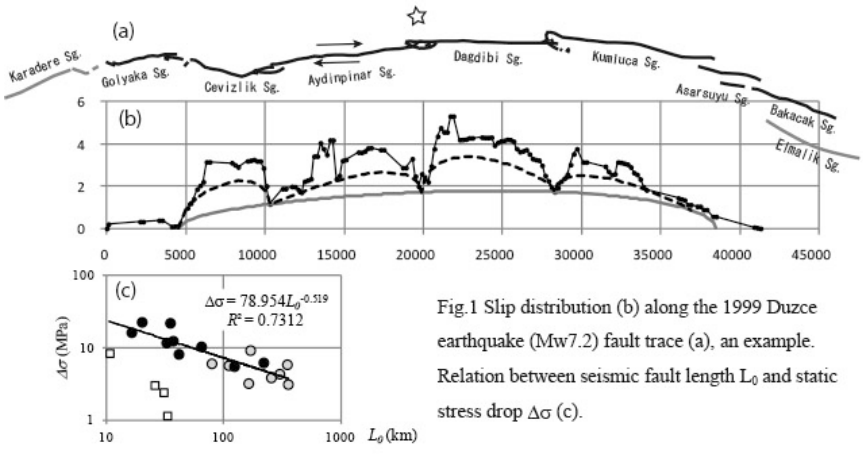

Fig.1 Slip distribution (b) along the 1999 Duzce earthquake (Mw7.2) fault trace (a), an example. Relation between seismic fault length L_0 and static stress drop $\Delta\sigma$ (c).

Japan Geoscience Union Meeting 2015
(May 24th - 28th at Makuhari, Chiba, Japan)

SSS30-07 Room:A05 Time:May 25 10:30-10:45

An arithmetic approach for modeling of seismic activity

FUJIWARA, Hiroyuki[1*]

[1]NIED

The ”arithmetic seismic activity model” is proposed by Fujiwara (2014) and the seismic activity is modeled by using the prime numbers to express the seismic activity that follows the G-R law as mathematical model. Although the ”arithmetic seismic activity model” is one that has been inferred from the phenomenological similarities between seismic activities and the prime number distributions, there may be some mathematical and physical meanings behind the model. Focusing on the relationship called trace formula, a study have been conducted.

We consider a correspondence between earthquakes and prime numbers. We parameterize occurrence time of earthquakes as the prime numbers and magnitude of earthquakes as the interval of prime numbers. Then we obtain a relationship similar to G-R law. We call the model obtained by this correspondence as ”arithmetic seismic activity model”. In the ”arithmetic seismic activity model”, earthquake is equivalent to prime number. Earthquake prediction is equivalent to prediction of emergence of prime numbers.

Trace formula is an equation obtained by calculating the trace of certain operator in two ways. A common feature in the trace formula, the sum on the prime elements in the geometric side is equal to the sum on the eigenvalues in the spectrum side. By generalizing these characteristics of the trace formula, it is possible to regard the explicit formula on prime numbers obtained by Riemann as one of the trace formula. Point processes in which points are irregularly occurred are difficult to handle in mathematical modeling. By using the trace formula, however, it is possible to express a point process as a sum of relatively simple continuous functions. Thus, by using the trace formula, an irregular point process is expected to be modeled as an eigenvalue problem of certain dynamical system.

An earthquake is understood as a phenomenon that corresponds to a change in the energy level of the field. Using certain quantum system, we consider to model a field of earthquake occurrence. Considering a Hamiltonian of the field of earthquake occurrence, we set earthquake occurrence as an eigenvalue problem for the Hamiltonian. If we can show that the eigenvalue problem is associated with the zeta function, we can expect to explain the similarity between the distribution of the prime and seismic activity. At present, any dynamical systems can explain seismic field based on this concept are not known. On the other hand, researches on the distribution of prime numbers are progressing to try to understand the distribution of zeros of the Riemann zeta function, which is equivalent to the distribution of prime number, as an eigenvalue problem of a quantum dynamical system.

Connes derived a trace formula of Selberg type by considering the operation of an idele class group on a square integrable function space that is defined on a space of adele class and showed that to prove the trace formula and to prove the Riemann conjecture are equivalent. Volovich proposed the p-adic quantum mechanics and considered an extension of quantum mechanics onto an adele space. As a part of their research, harmonic oscillators on an adele space are introduced and the Mellin transforms of them are shown to be expressed using the Riemann zeta function. Thus, eigenvalue problems of dynamical systems that are configured on an adele space are found to be associated naturally with the Riemann zeta function.

In this study, referring to the idea of extension of the quantum mechanics onto an adele space, we try to formulate the quantization (non-commutativization) of the continuum mechanics that gives the physical basis of seismology. On the basis of these basic studies, an attempt is made to regard earthquake oocuurence as eigenvalue problems of dynamical systems on an adele space.

Keywords: number theory, prime number, earthquake, trace formula, adele

Japan Geoscience Union Meeting 2015
(May 24th - 28th at Makuhari, Chiba, Japan)

SSS30-08 Room:A05 Time:May 25 11:00-11:15

Systematic Understanding of Dynamic Earthquake Slip Process in the System without Fluid Flow

SUZUKI, Takehito[1*] ; YAMASHITA, Teruo[2]

[1]Coll. Sci. & Eng., AGU, [2]ERI, Univ. Tokyo

We have explained many aspects of dynamic earthquake slip process by constructing the framework associated with the interaction among heat, fluid pressure and inelastic pore creation. We found three nondimensional parameters, Su, Su' and Ta, in the framework. In particular, Su describes the relative dominance of the effect of inelastic pore creation on the fluid pressure change over that of shear heating. In our previous studies, we analyzed the parameter range $Su>1-v_0^*$, where v_0^* is the initial value of the normalized slip velocity v^*. For this parameter range, we found the acceleration case and the spontaneous slip cessation case for the slip process. The acceleration case shows the transition from deceleration to acceleration with high-speed final slip, while the spontaneous slip cessation case shows the slip arrest with final zero stress drop. The former case corresponds to gradual acceleration phase (GAP) or a dynamic event preceding the main shock, while the latter indicates pulse-like slip for 2-D fault models. They are quantitatively distinguished by the value of the function G; if $G>0$, the acceleration case is observed, while if $G<0$, the spontaneous slip cessation case appears. We assume the parameter range $Su<1-v_0^*$ in the present study.

First, we found that the steady state value of the normalized slip velocity is zero or unity over a whole range of Su. In addition, deceleration at the initial stage of the slip is required to attain the steady state value zero. In the case $Su<1-v_0^*$, we found analytically that temporal differentiation of slip velocity is always positive, which leads to the conclusion that only acceleration occurs (the steady state value unity is realized) during the slip.

In this case, thermal pressurization is predominant over the pore creation, so that high-speed slip and complete stress drop are observed. Moreover, temperature increase is kept below the fault rock melting point. We found that these natures describe slip for the ordinary earthquakes with GAP and the high-speed slip and without the fault rock melting, which is the same behavior as those of $Su>1-v_0^*$ and $G>0$. It is also important here that, since the final porosity is less than the upper value, we can reproduce (i) non-negligible porosity generation, and (ii) temperature under the fault rock melting point, both of which have been seismologically fundamental requirements, as done in the case $Su>1-v_0^*$. The behavior in the system without the fluid flow is understood in a unified way for all values of Su.

Keywords: theory, heat, fluid pressure, pore creation, nonlinear, interaction

Japan Geoscience Union Meeting 2015
(May 24th - 28th at Makuhari, Chiba, Japan)

SSS30-09 Room:A05 Time:May 25 11:15-11:30

Generation of low-frequency tremor by fluid flow

SAKURABA, Ataru[1*]

[1]School of Science, University of Tokyo

We discuss the possibility that flow-induced instability along underground conduit or plane layer causes low-frequency tremor. One example is generation of volcanic tremor, which occurs before or during eruption and lasts more than a few minutes with oscillation period of 0.2-2 seconds (e.g., see Konstantinou and Schlindwein, *J. Volcanol. Geotherm. Res*., 2002). Sakuraba and Yamauchi (*Earth Planets Space*, 2014) showed that a relatively slow magma flow speed of O(1) m/s through a plate-like dike of thickness of around 0.5 m can cause linear instability in flow perturbation and surrounding elastic wave field. The critical magma flow speed decreases in inverse proportion to the Rayleigh-wave wavelength propagating along the dike with flexural deformation. They concluded that natural dike lengths put constraint on the oscillation period, but a subsequent study suggests that a finite dike width may determine the longest wavelength that allows instability. A laboratory experiment is also ongoing to verify the above theoretical prediction that a viscous fluid flow through a plate-like conduit can create self-oscillations. Another example may be found in generation of non-volcanic deep tremor that occurs at subducting plate (Obara, *Science*, 2002). This is still a speculation motivated from a study by Kumaran, Fredrickson and Pincus (*J. Phys. II France*, 1994) who considered Couette flow between two parallel plates, one of which is rigid and the other is moving, but the medium between the plates is two-layered: a fluid layer is placed on a layer of soft (viscoelastic) material. They theoretically showed that flow-induced vibration can occur with a very small shear rate. In an idealized situation in which the solid layer extends infinitely, the critical speed of the moving plate decreases in inverse proportion to the characteristic length scale of the associated wave that propagates at a half the plate speed. Though we have not examined whether this model explain time scales of observations with reasonable physical and material properties, similarity between the above mentioned examples suggests that flow-induced instability may explain some of the tremor events.

Keywords: flow-induced vibration, volcanic tremor, non-volcanic deep tremor

Japan Geoscience Union Meeting 2015
(May 24th - 28th at Makuhari, Chiba, Japan)

SSS30-10 Room:A05 Time:May 25 11:30-11:45

High-resolution tremor locations reveal behaviors of secondary slow slip fronts in the context of the main front

PENG, Yajun[1*] ; RUBIN, Allan[1]

[1]Department of Geosciences, Princeton Univeristy

Non-volcanic tremor is generally interpreted as the seismic manifestation of slow slip, and tremor locations have been used extensively to infer detailed behaviors of slow slip fronts due to higher spatial and temporal resolution over geodetic observations. Taking advantage of S-wave coherence among stations separated by roughly 10 km, we obtain high precision tremor locations in Cascadia using cross-station cross correlations, with either 3-station detectors (southern Vancouver), or 3-array detectors (Olympic Peninsula). We observe that near the main front, tremor migrations usually propagate along the main front, regardless of its orientation, and their recurrence intervals are too short to be tidally driven. Rapid tremor reversals (RTRs) originate from the main front, and sometimes start as migrations propagating along the main front. Although the occurrence of most of the RTRs appears to be correlated with high tidal shear stresses, we observe a few exceptions, which may suggest that the stress increase far behind the main front induced by secondary fronts at the main front is sometimes enough to initiate a RTR. Beneath Olympic peninsula, the spatial densities of tremor during the ETS and the inter-ETS events seem to be complementary, and RTRs do not often extend into regions that are de-stressed by the inter-ETS event.

Preliminary results of tremor locations beneath Guerrero, Mexico indicate that our method also performs well in this region. It seems that a tremor asperity about 50 km across ruptured quasi-periodically with a recurrence interval of ˜3 months until the 2006 slow slip event drastically decreased it.

Keywords: Episodic tremor and slip, Cascadia subduction zone, Mexican subduction zone, Cross-station method

Japan Geoscience Union Meeting 2015
(May 24th - 28th at Makuhari, Chiba, Japan)

SSS30-11 Room:A05 Time:May 25 11:45-12:00

Source parameters of foreshocks and aftershocks of 2014 Northern Nagano earthquake

IMANISHI, Kazutoshi[1*] ; UCHIDE, Takahiko[1]

[1]Geological Survey of Japan, AIST

The 2014 M6.7 Northern Nagano earthquake occurred on 22 November, 2014, which broke a part of Kamishiro fault. In order to reveal the generation mechanism of the mainshock, we determined hypocenters and source parameters of foreshock sequence from four days before the mainshock, as well as aftershocks.

We assumed two different one-dimensional crustal velocity structures to account for heterogeneous velocity structure in the studied area. Hypocenters are shifted by the relocation to the east at about 2 km and shallower at most 5 km, compared with the JMA catalogue. Although the aftershock distribution basically defines an eastward dipping plane, vertical and westward dipping planes are also identified at the middle to the northern part of the source region. The foreshocks located at about 3 km depth and distributed on NNW dipping plane, which is clearly distinct from the aftershock distribution. It is noted that the foreshock sequence started at the deeper part, then migrated to the shallower part and finally approached to the mainshock nucleation point.

We then determined focal mechanisms from P-wave polarity data as well as body wave amplitude, which enabled us to obtain well-determined solutions down to M0.5. Most of aftershocks exhibit a large strike-slip component, while aftershocks occurring at the southern part of the source region show reverse faulting type of mechanisms. This feature is consistent with the aftershock distribution. As for the foreshock sequence, we obtained a number of events with a large strike-slip component having a nodal plane dipping to the NNW, which is also consistent with the foreshock distribution. Interestingly, we found that the foreshock focal mechanisms slightly change with time and finally resemble to the P-wave first-motion mechanism of the mainshock. We detected more than 400 new events based on visual inspection of running spectra and S-P time at the station closest to the foreshock sequence (Hi-net Hakuba station). Hypocenter and focal mechanism determination of these events will further contribute to elucidate the relation between the foreshock sequence and the mainshock occurrence.

We will also present the stress drop estimations and discuss the spatial distribution of stress drops as well as the difference in source properties between the foreshocks and aftershocks.

Acknowledgements: Seismograph stations used in this study include permanent stations operated by NIED (Hi-net), JMA, ERI, and DPRI.

Keywords: Northern Nagano earthquake, source parameter, foreshock, aftershock

Japan Geoscience Union Meeting 2015
(May 24th - 28th at Makuhari, Chiba, Japan)

SSS30-12 Room:A05 Time:May 25 12:00-12:15

Source process of the 2014 Northern Nagano earthquake

KOBAYASHI, Hiroaki[1*] ; KOKETSU, Kazuki[1] ; MIYAKE, Hiroe[1]

[1]Earthquake Research Institute, University of Tokyo

An earthquake with JMA magnitude 6.7 occurred on 22 November, 2014, in the northern Nagano prefecture, Japan. This earthquake caused 46 casualties and damaged over 1500 housings. GCMT, F-net and JMA-CMT solution are coincide with each other and shows that a focal mechanism of this earthquake is reverse fault with some strike-slip components and about 20% non-DC component. Immediately after the earthquake, various institutions conducted field surveys and reported surface faults. Because the surface fault traces mostly matched with a known active fault named the Kamishiro fault, this fault is thought to be ruptured during the earthquake. The Kamishiro fault is located at the northern part of the Itoigawa-Shizuoka Tectonic Line which is one of the largest fault zones in Japan. It is important to investigate the source process of the earthquake. We performed a joint inversion of strong-motion and geodetic data to understand the source process of the earthquake.

In the northern Nagano region, there are dense strong-motion observation networks of K-NET, KiK-net, SK-net, and ERI. We used 45 components at 15 stations for the source inversion. All the waveforms were integrated to velocity, band-pass filtered between 0.02 - 0.4 Hz, and resampled with 0.25 s. For geodetic data, we chose 9 stations from GEONET. We used the daily coordinates of the F3 solution (Nakagawa et al., 2009) of GSI. To calculate static displacement by the earthquake, we set GEONET Shirotori as a reference point and then compared the mean value of 2-6 days before and after the earthquake. We used horizontal components and three components for GEONET Hakuba where significant vertical displacement was observed.

We used inversion methods of Yoshida et al. (1996) and Hikima and Koketsu (2005). Strong-motion Green's functions were calculated by the method of Kohketsu (1985) with one-dimensional velocity structure model based on the Japan Integrated Velocity Structure Model [JIVSM] (Koketsu et al., 2008, 2012) for each station. Geodetic Green's functions were calculated by the method of Zhu and Rivera (2002). In this calculation, a one dimensional velocity structure model beneath the GEONET Hakuba was extracted from the JIVSM and used for all the stations. We divided the faults into 13 x 7 subfaults and set strike and dip angles considering the surface faults and aftershock distributions. Each subfault has a size of 2 km x 2 km with a point source at the center with rake angle of 45±45 to represent from reverse to left-lateral strike-slip faulting.

We obtained largest slip located at the north-eastern deeper part of the hypocenter. The shallower part has also some slips with maximum at near GEONET Hakuba. This slip area coincides with the observed largest surface displacement point. However, the focal mechanism calculated by summing up obtained slip vectors cannot explain the non-DC component, suggesting further investigation needed.

Keywords: 2014 Northern Nagano earthquake, source process, source inversion

Japan Geoscience Union Meeting 2015
(May 24th - 28th at Makuhari, Chiba, Japan)

SSS30-13 Room:A05 Time:May 25 12:15-12:30

Dynamic rupture model of the 2014 northern Nagano, central Japan, earthquake

KASE, Yuko[1*]

[1]Geological Survey of Japan, AIST

The 2014 northern Nagano, central Japan, earthquake (M_{JMA}6.7) occurred in November 22, 2014. The surface ruptures intermittently observed along the Kamishiro fault (Katsube, this meeting), but the southern part of the fault remains to be ruptured. We construct a dynamic rupture model of the earthquake to understand the mechanism of the earthquake and the present condition of the fault.

Fault length and lower depth of the fault is 22 km and 15 km, respectively, based on the aftershock distribution (JMA, 2014; NIED, 2014) and InSAR image (GSI, 2015). Fault strike is N10E, based on the aftershock distribution and the strike of the Kamishiro fault (MEXT et al., 2004). Dip angle of the deeper region than 2 km is 60 degrees, based on the CMT solutions (JMA, 2014; NIED, 2014) and aftershock distribution, and dip angle of the shallower region than 2 km is 45 degrees, based on the analysis of the InSAR data (Yarai, 2015). The southern part of the fault reaches the earth's surface, while upper depth of the northern part is 2 km. Principal stresses are proportional to depth. Azimuth of the maximum principal stress is N65W (MEXT et al., 2004). The minimum principal stress is vertical, and equal to overburden load. We assume hydrostatic condition. The medium has 2-layered structure with 2 km-depth boundary, based on the subsurface structure model around the fault (NEID, 2003). The upper layer has zero stress drop, since it corresponds to sediment layer. We calculate dynamic rupture processes by the finite-difference method (Kase, 2010), assuming the slip-weakening friction law, and search average stress drop that is consistent with the observed seismic moment.

In case that the average stress drop is 3.3 MPa, the seismic moment is 6.21 x 10^{18} Nm (Mw6.5), which is almost agree with the CMT solutions. Rupture first smoothly propagates, because our dynamic rupture model is laterally homogeneous. After the rupture reaches 2 km-depth, the rupture suddenly decelerates because of zero stress drop. The maximum slip on the fault is about 2 m, and the maximum surface slip is about 1.1 m, which is agree with the observed one (Hirouchi et al., 2014).

Keywords: dynamic rupture, 2014 northern Nagano earthquake, Kamishiro fault, numerical simulation

Japan Geoscience Union Meeting 2015
(May 24th - 28th at Makuhari, Chiba, Japan)

SSS30-14 Room:A05 Time:May 25 14:15-14:30

Fault strength in Marmara region inferred from the geometry of the principle stress axes and fault orientations

PINAR, Ali[1*] ; COSKUN, Zeynep[1] ; MERT, Aydin[1] ; KALAFAT, Dogan[1]

[1]Bogazici University Kandilli Observatory and Earthquake Research Institute

The general consensus based on historical earthquake data suggests that the last major moment release on the Prince's islands fault was in 1766 which in turn points out an increased seismic risk for Istanbul Metropolitan area considering the fact that most of the 20 mm/yr GPS derived slip rate for the region is accommodated mostly by that fault segment.

The orientation of the Prince's islands fault segment overlaps with the NW-SE direction of the maximum principle stress axis derived from the focal mechanism solutions of the large and moderate sized earthquakes occurred in the Marmara region. As such, the NW-SE trending fault segment translates the motion between the two E-W trending branches of the North Anatolian fault zone; one extending from the Gulf of Izmit towards C?narc?k basin and the other extending between offshore Bak?rkoy and Silivri.

The basic relation between the orientation of the maximum and minimum principal stress axes, the shear and normal stresses, and the orientation of a fault provides clue on the strength of a fault, i.e., its frictional coefficient. Here, the angle between the fault normal and maximum compressive stress axis is a key parameter where fault normal and fault parallel maximum compressive stress might be a necessary and sufficient condition for a creeping event. That relation also implies that when the trend of the sigma-1 axis is close to the strike of the fault the shear stress acting on the fault plane approaches zero. On the other hand, the ratio between the shear and normal stresses acting on a fault plane is proportional to the coefficient of frictional coefficient of the fault. Accordingly, the geometry between the Prince's islands fault segment and a maximum principal stress axis matches a weak fault model.

Keywords: stress tensor, fault orientation, frictional coefficient

Japan Geoscience Union Meeting 2015
(May 24th - 28th at Makuhari, Chiba, Japan)

SSS30-15 Room:A05 Time:May 25 14:30-14:45

High-frequency falloff exponent of source spectra: Case of Fukushima-Hamadori and northern Ibaraki area

UCHIDE, Takahiko[1*] ; IMANISHI, Kazutoshi[1]

[1]Geological Survey of Japan, AIST

The moment spectra, often referred to as the source spectra, have been investigated to characterize the earthquake source processes. The omega-square model has often worked as the standard model for the source spectra. The model has flat spectra in the lower frequencies and the falloff proportional to ω^{-2}, where ω is angular frequency, in the higher frequencies. The corner frequency dividing those two frequency bands represents the inverse of the source duration and therefore indicates the source size and then the representative stress drop.

The high-frequency falloff exponent is also an important source parameter. Although 2 of the exponent is often applicable, the exponent other than 2 is sometimes reported [e.g., Venkataraman et al., 2006; Allmann and Shearer, 2009]. Uchide et al. [SSJ Fall Meeting, 2014] found 1.6 of it in Hamadori (Coastal area) of Fukushima Prefecture and northern Ibaraki Prefecture, northeast Japan, by the stacking method [Shearer et al., 2006], while 2 worked well in the Tohoku-oki area, northeast Japan [Uchide et al., JGR, 2014]. This result must be confirmed by other method, therefore we here study the spectral ratio between target events and smaller events nearby (hereafter referred to as "empirical Green's function (EGF) event"), focusing on the high-frequency falloff exponent.

In order to stabilize the result, we obtain the spectral ratios using multiple time window [Imanishi and Ellsworth, 2006]. In addition, we stack the spectral ratios from multiple stations and all three components by taking the median spectral ratio at each frequency. Then we grid-search the high-frequency falloff exponent in addition to the corner frequencies of both the target and EGF events, and the seismic moment ratio of those events.

In fact, it is difficult to constrain the high-frequency falloff exponent from a single spectral ratio, since there is the trade-off between the corner frequency and the falloff exponent. Therefore we simultaneously fit the spectral ratios between the specific target and different EGF events, assuming the common corner frequency of the target event and the common falloff exponent for the target and EGF events. The preliminary result implies the high-frequency exponent less than 2.0 for some events, while some other events prefer 2.0 of the exponent. Finally we will discuss the cause of the variation in the high-frequency falloff exponent.

Keywords: earthquake, spectral study, spectral ratio

Japan Geoscience Union Meeting 2015
(May 24th - 28th at Makuhari, Chiba, Japan)

SSS30-16 Room:A05 Time:May 25 14:45-15:00

Earthquake cluster activity beneath Tanzawa Mountains in 2012: Migration with a small stress drop

YAMADA, Takuji[1*] ; YUKUTAKE, Yohei[2] ; TERAKAWA, Toshiko[3] ; ARAI, Ryuta[4]

[1]Inst. Seismol. and Volc., Hokkaido Univ., [2]Hot Springs Res. Inst. of Kanagawa Pref., [3]Earthq. and Volc. Res. Center, Nagoya Univ., [4]Japan Agency Marine-Earth Science and Technology

An earthquake cluster activity took place beneath the Tanzawa Mountains, which is located NE of Mt. Fuji, Japan, with a depth of 20 km at the end of January, 2012. The activity began at 22:39 UT on 27 January and included 78 earthquakes with M $\geq$ 2.0 in the area within 50 hours. Five of them had magnitudes greater than 4.0 and the largest one was M5.4.

First we relocated hypocenters by using the double difference method and found that earthquakes of the cluster activity migrated away from the first earthquake of the activity. The migration was consistent with the fluid diffusion and could be characterized as following two patterns. Earthquakes that occurred within an hour of the first earthquake had a migration speed similar to that of non-volcanic tremors. On the other hand, those occurred between an hour and 50 hours from the first earthquake of the activity showed a migration with a similar speed to the activity of induced earthquakes due to water-injection experiments. These results suggest that the cluster activity would be triggered by a slow slip and fluid diffusion. We confirmed that this migration would not be an apparent one by numerical simulations.

We then analyzed stress drops of 16 earthquakes with M $\geq$ 3.5 that occurred from July, 2003 to June, 2012 in the area of the activity. Earthquakes that occurred before and after the cluster activity had stable values of stress drop with 30 MPa estimated by the equation of Madariaga (1976), or 5 MPa by Brune (1970). On the other hand, earthquakes of the cluster activity included ones with significantly small stress drops. A hypothesis that the cluster activity was associated with fluid explains both the migration of hypocenters and small stress drops of the cluster activity. This is because the shear strength on a fault can be decreased due to the pore pressure of the fluid. This hypothesis is also supported by the fact that earthquakes before and after the cluster activity had similar values of stress drop and that structural studies indicated the existence of little fluid in the region, suggesting that the activity was triggered by a different mechanism from the other earthquakes in the same region. The most plausible explanation is that there is a little fluid in a closed system beneath the Tanzawa Mountains which is undetectable by structural observations.

Acknowledgments: We used waveforms at stations of Hi-net (NIED), Hot Spring Research Institute of Kanagawa Prefecture, Univ. of Tokyo, and JMA, as well as the seismograph network called the MeSO-net, which has been developed under the “Special Project for Earthquake Disaster Mitigation in the Tokyo Metropolitan Area” since 2007. We also used arrival times of P and S waves determined by JMA. Figures were created using Genetic Mapping Tool.

Keywords: Tanzawa Mountains, earthquake cluster activity, migration, stress drop, fluid, pore pressure

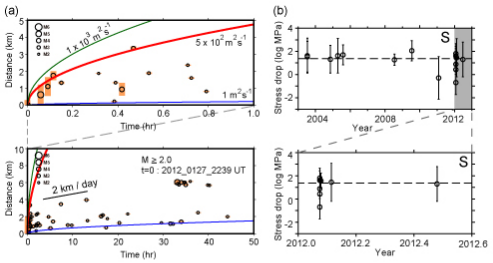

Fig. (a) Hypocentral distances from the first earthquake as a function of elapsed time less than an hour and 50 hours, with scales of source radii. Vertical orange bars indicate source dimensions calculated from estimated stress drops by S waves. Red curve with a diffusivity of 5.0 x 10^{2} m^{2} s^{-1} explains the data better than the other values (green and blue lines) for time < 1 hr. The seismicity for 1 ≤ time ≤ 50 hrs shows a migration with a speed of 2 km a day. (b) Estimated stress drops from S waves as a function of time. Black horizontal broked lines indicate average stress drops of earthquakes that occurred before and after the cluster activity. Results after January 2012 are also shown in the lower panel.

Japan Geoscience Union Meeting 2015
(May 24th - 28th at Makuhari, Chiba, Japan)

SSS30-17 Room:A05 Time:May 25 15:00-15:15

Resistivity structure and 3He/4He ratios around the focal zone of the 2011 Mw 5.9 earthquake beneath Mt. Fuji, Japan

AIZAWA, Koki[1*] ; SUMINO, Hirochika[2] ; UYESHIMA, Makoto[3] ; YAMAYA, Yusuke[4] ; HASE, Hideaki[5] ; OHNO, Masao[1] ; TAKAHASHI, Masaaki[4] ; KAZAHAYA, Kohei[4] ; RUNG-ARUNWAN, Tawat[6] ; OGAWA, Yasuo[7]

[1]Kyushu University, [2]Geochemical Research Center, Graduate School of Science, University of Tokyo, [3]ERI, University of Tokyo, [4]AIST, [5]GERD, [6]Mahidol University, [7]KSVO, TITECH

We present the results of a joint 3-D resistivity and isotopic analysis of the groundwater system surrounding Mt. Fuji, Japan, where increased seismicity was observed following the 2011 TohokuOki megathrust earthquake. The electrically conductive zone and high concentrations of magmatic helium correspond to this zone of triggered seismicity. In contrast, 2H (D) and 18O isotope ratios, and Li/Cl ratios do not support the presence of magmatic water. These results suggest that the earthquakes were triggered within a fractured zone where only magmatic gas preferentially travels upward. Although multiple mechanisms may jointly contribute to this remote earthquake generation, we hypothesize that a small fraction of gas bubbles, which are originally secured within the fracture zone by capillary trapping, play a key role for earthquake triggering.

Japan Geoscience Union Meeting 2015
(May 24th - 28th at Makuhari, Chiba, Japan)

SSS30-18 Room:A05 Time:May 25 15:15-15:30

Spatial variation of seismic radiation properties for large interplate earthquakes in northeast Japan

KUBO, Hisahiko[1*] ; IWATA, Tomotaka[2] ; ASANO, Kimiyuki[2] ; AOI, Shin[1]

[1]National Research Institute for Earth Science and Disaster Prevention, [2]Disaster Prevention Research Institute, Kyoto University

Kubo et al. (2014, AGU) constructed kinematic source models for the 2011 Tohoku-oki earthquake (M_w 9.1) in multi successive period-bands using strong-motion data, and discussed the period-dependent seismic radiation and broadband source characteristics for this event based on the spatial difference of the slip velocity function for each period-band. This multi period-band source modeling has an advantage that this method provides the direct comparison among source models in multi period-bands. In this study, we investigate the period-dependent seismic radiation for the 2011 Ibaraki-oki earthquake (M_w 7.9), which is the largest aftershock of the 2011 Tohoku-oki earthquake, using the same procedure as Kubo et al. (2014, AGU) in order to compare the rupture behaviors of these earthquakes and take the first step for the discussion on the spatial variation of seismic radiation properties for large interplate earthquakes in northeast Japan.

The analysis period-bands for the 2011 Ibaraki-oki earthquake is 5-10 s, 10-25 s, and 25-50 s. The source model for each period-band is estimated by the fully Bayesian kinematic source inversion with the multi-time-window method (Kubo et al., 2014, SSJ). Three components of strong-motion velocity waveforms at 15 stations of K-NET, KiK-net, and F-net of NIED are used in this analysis. Green's functions are calculated by the FDM (GMS; Aoi & Fujiwara, 1999) with a 3D velocity structure model (JIVSM; Koketsu et al., 2012). The validity of the 3D velocity structure model used for the 3D Green's functions was confirmed through waveform comparisons for M~6 events. A curved fault model is constructed based on the shape of the plate boundary of JIVSM, and then is divided into 144 subfaults of approximately 10 km $\times$ 10 km. The slip time history of each subfault is represented by a series of nine smoothed-ramp functions with 4.0 s width, each of which is put with 2.0 s lag. The first time-window triggering velocity of 2.0 km/s is selected so as to minimize the residual of strong-motion data fitting in the period-band of 5-50 s.

The estimated rupture process in the period-band of the 5-10 s differs from those estimated in the period-bands of 10-25 s and 25-50 s. The source models in period-bands of 10-25 s and 25-50 s have large slips in the shallow area south and southeast of the hypocenter, while large slips for the source model in the period-band of 5-10 s are located in the deep area which is approximately 30 km west of the hypocenter. This means that these regions mainly radiated the long-period (10-25 s and 25-50 s) and relatively-short-period (5-10 s) waves, respectively. These results indicate that the 2011 Ibaraki-oki earthquake had an along-dip variation in its seismic radiation, which is consistent with the along-dip segmentation of interplate fault suggested by Lay et al. (2012).

The comparison of the results for the 2011 Tohoku and the 2011 Ibaraki earthquakes indicates that the seismic radiation for both events was segmented along the dip direction: short- and long-period seismic waves were predominantly radiated from the deep and shallow regions, respectively. However, the deep off-Miyagi region during the 2011 Tohoku earthquake radiated not only short- but also long-period waves, and this implies the possibility of the spatial variation of seismic radiation property in northeast Japan. This is also supported by previous studies which have noted different seismic radiation properties among other large interplate earthquakes in the northeast Japan, although the details of the seismic radiation for the other earthquakes are not clear and it is necessary to apply the multi period-band source modeling to these events.

[Acknowledgments] The strong-motion data recorded by K-NET, KiK-net, and F-net of NIED was used for this analysis.

Keywords: Spatial variation of seismic radiation property, Large interplate earthquakes in northeast Japan, Multi period-band source modeling, Strong-motion data, The 2011 Tohoku-oki earthquake, The 2011 Ibaraki-oki earthquake

Japan Geoscience Union Meeting 2015
(May 24th - 28th at Makuhari, Chiba, Japan)

SSS30-19 Room:A05 Time:May 25 15:30-15:45

Randomness of megathrust earthquakes implied by rapid stress recovery after the 2011 Tohoku-oki earthquake

TORMANN, Thessa[1] ; ENESCU, Bogdan[2*] ; WOESSNER, Jochen[1] ; WIEMER, Stefan[1]

[1]ETH Zurich, Swiss, [2]Faculty of Life and Environmental Sciences, University of Tsukuba

Constraining the recurrence of megathrust earthquakes is genuinely important for hazard assessment and mitigation. The prevailing approach to model such events worldwide relies on the segmentation of the subduction zone and quasi-periodic recurrence due to constant tectonic loading. In this study, we have used the earthquake catalog of the Japan Meteorological Agency (JMA) and analyzed events recorded along a 1,000-km-long section of the subducting Pacific Plate beneath Japan since 1998 to map the relative frequency of small to large earthquakes, expressed by the slope of the frequency-magnitude distribution of earthquakes (the so-called b-value). Evidence from laboratory experiments, numerical modeling and natural seismicity indicates that the b-value is negatively correlated with the differential stress.

Our analysis reveals that the spatial distribution of b-values reflects well the tectonic processes accompanying plate motion. However, there is no evidence of distinct earthquake-generation regions along the megathrust, associated with the so-called ”characteristic earthquakes”.

Nevertheless, we show that parts of the plate interface that ruptured during the 2011 Tohoku-oki earthquake were highly stressed in the years leading up to the earthquake, as expressed by mapped, very low regional b-values. Although the stress was largely released during the 2011 rupture, thus leading to an increase in b-values immediately after the megathrust event, the stress levels (i.e., b-values) quickly recovered to pre-megaquake levels within just a few years. This suggests that the megathrust zone is likely ready for large earthquakes any time with a low but on average constant probability.

Our results imply that large earthquakes may not have a characteristic location, size or recurrence interval, and might therefore occur more randomly distributed in time. The findings also bring strong evidence that the size distribution of earthquakes is sensitive to stress variations and its careful monitoring can improve the seismic hazard assessment of the megathrust zone.

Reference:
Thessa Tormann, Bogdan Enescu, Jochen Woessner, Stefan Wiemer, Randomness of megathrust earthquakes implied by rapid stress recovery after the Japan earthquake, *Nature Geoscience*, **8**, 152-158, doi:10.1038/ngeo2343, 2015.

Keywords: Tohoku-oki earthquake, earthquake cycle, seismicity, b-value, differential stress

Japan Geoscience Union Meeting 2015
(May 24th - 28th at Makuhari, Chiba, Japan)

SSS30-20 Room:A05 Time:May 25 16:15-16:30

Radiated and Frictional Energy of the 2011 Tohoku-oki Earthquake

MORI, James[1*]

[1]Kyoto University DPRI

The Japan Trench Fast Drilling Project (JFAST) estimated the level of dynamic friction on the shallow portion of the fault that had the very large slip during the 2011 Tohoku-oki earthquake. From both laboratory experiments on the fault zone material and temperature measurements across the fault zone, the shear stress during the earthquake rupture was estimated to be about 0.6 MPa at 820 meters below the sea floor (including the water depth this is equivalent to about 3. 5 km of rock overburden). This shear stress corresponds to a coefficient of friction of about 0.1. Combining these results with estimates of the radiated energy, show that the ratio of frictional heat to radiated energy is less than 1.0 for the shallow portion of the fault. These estimates are related to the large slip portion of the earthquake in the shallow region of the megathrust and are not representative of the deeper portions of the earthquake rupture area. Averages for the whole earthquake suggest that the ratio of frictional heat to radiated energy is much larger (about 10) and similar to values inferred for typical earthquakes. This implies there is a significant difference in the energy partition between the shallow portion (with large slip) and the deeper portions (moderate slip) of the subduction fault. The shallow/deep portion of the fault produces relatively more/less radiated energy compared to the frictional heat.

Keywords: earthquake source, energy, Tohoku-oki earthquake, friction, radiated energy

Japan Geoscience Union Meeting 2015
(May 24th - 28th at Makuhari, Chiba, Japan)

SSS30-21 Room:A05 Time:May 25 16:30-16:45

Estimation of Radiated Seismic Energy of Repeating Earthquakes in Northeastern Japan and its Spatio-Temporal Variation

ARA, Masamichi[1*] ; IDE, Satoshi[1] ; UCHIDA, Naoki[2]

[1]The Univ. of Tokyo, [2]Tohoku University

Seismic activity on the plate interface is spatially heterogeneous. In addition to ordinary earthquakes of different sizes, tsunami earthquakes and slow earthquakes occur with much longer duration expected from the scaling relation of ordinary earthquakes. However, for example, the source areas of tsunami earthquakes are known to be located at shallower part of plate interface. Additionally, in the source area of the Tohoku-Oki earthquake, more high frequency seismic wave was radiated at deeper region of the plate interface [Ide et al., 2011]. Therefore, the fault property of the plate interface in the Tohoku-Oki region can be spatially heterogeneous. The spatial heterogeneity on the plate interface may result in the variation of radiated seismic energy, which conveys the information of dynamic rupture process. Among various earthquakes occurring near the plate interface, repeating earthquakes are relatively easy to understand because of its simple mechanism, as repeated slips of a small locked region of the plate interface to catch up with aseismic slip in surrounding region. Since, repeating earthquakes are considered to occur on the plate interface certainly, they are ideal targets to constrain the physical mechanism of brittle rupture on the plate interface. Many repeating earthquakes have been detected in the Tohoku-Oki region. The size and inter-event time of some repeating earthquake groups changed after the Tohoku-Oki earthquake. To examine the possible change of source process after the Tohoku-Oki earthquake can also contribute to the understanding of physical process of earthquakes. In this study, we estimated the radiated seismic energy of repeating earthquakes in the Tohoku-Oki region and examined its spatio-temporal variation.

The target earthquakes of this study are 160 repeating earthquakes detected by Uchida and Matsuzawa [2013]. These earthquakes are divided into 52 repeating earthquake groups. Seismic activity of these events extends before and after the Tohoku-Oki earthquake and includes groups that showed enlarged magnitude and shortened inter-event time after the earthquake as represented by Kamaishi sequence. To estimate radiated seismic energy, we use the method for measuring amplitude developed by Mayeda et al. [2003] and the method for estimating source spectra and radiated seismic energy developed by Baltay et al. [2010] with slight modifications. In this modification, we linearized the calculation to quantitatively estimate the error of the radiated seismic energy that has not been discussed precisely.

We obtained a positive depth dependency of scaled energy, the ratio between radiated seismic energy and seismic moment, as a main characteristic of spatial variation. This is consistent with the results in previous studies. We also observe some temporal changes in scaled energy. For Kamaishi-sequence, the scaled energy decreased suddenly after the Tohoku-Oki earthquake and gradually recovered, coinciding with a sudden increase and gradual decay of seismic moment. This temporal change of seismic moment has been interpreted as the expansion of rupture into conditionally stable region around the unstable region [Uchida et al., 2015]. The temporal change of scaled energy suggests that the ratio of fracture energy is larger in this conditionally stable region.

Radiated seismic energy is related to the strength of the fault, which increases after an earthquake. Therefore, we expect some correlation between the inter-event time and scaling energy for repeating earthquakes. In our result, there are several groups and regions that have positive dependency of scaled energy on the inter-event time, but this relation cannot be confirmed generally.

Japan Geoscience Union Meeting 2015
(May 24th - 28th at Makuhari, Chiba, Japan)

SSS30-22 Room:A05 Time:May 25 16:45-17:00

Emergence, moment change and disappearance of small repeating earthquakes following the 2011 Tohoku earthquake

HATAKEYAMA, Norishige[1*] ; UCHIDA, Naoki[1] ; MATSUZAWA, Toru[1]

[1]Graduate School of Science, Tohoku University

Small repeating earthquakes, which occur repeatedly at almost the same location, are thought to represent repeated ruptures of a small seismic patch on a fault plane. There are many unknown features about repeaters such as detailed structures of the patch and causes of irregularity in the magnitude and the recurrence interval.

Some small repeating earthquake sequences show systematically increased seismic moments after the 2004 M6.0 Parkfield earthquake (Chen et al., 2010) and the 2011 M9.0 Tohoku earthquake (Tohoku EQ; Uchida et al., 2015) in the areas where large afterslip occurred. These phenomena can be explained by increases in rupture areas due to aseismic-to-seismic transitions at high loading rate in conditionally stable regions around the repeaters. Understanding slip behavior changes in conditionally stable regions due to stress perturbation is important for revealing the generation mechanisms of recurrent interplate earthquakes.

In this study, we performed hypocenter relocations in a small area off Miyako-city, Iwate-prefecture, Japan, to examine temporal changes in seismic activities before and after the Tohoku EQ. We selected a small area including a cluster of earthquakes with repeaters at a depth of ∼40km, corresponding to the depth to the plate boundary. A large afterslip of the Tohoku EQ was estimated to have occurred in this area (e.g., Ozawa et al., 2012).

We used the double-difference method (Waldhauser and Ellsworth, 2000) for the hypocenter relocation. Firstly, we relocated events around the cluster by using pick-data of the Japan Meteorological Agency to select earthquakes in the cluster for further analysis. Secondly, we precisely relocated events in the cluster by using travel-time differences estimated from waveform cross-spectra.

The results show that before the Tohoku EQ, M2.5-2.9 events (Group A) repeatedly occurred at almost the same location with quasi-periodic recurrence intervals (9-12 months). There were no events whose magnitudes were larger than 2.0 within 5km from the repeaters.

After the Tohoku EQ, three significant changes were observed in the seismic activities in the cluster.

(1) At the location where the Group-A events had occurred before the Tohoku EQ, earthquakes larger than M3.0 started to occur repeatedly. The recurrence intervals were much shorter than before (eleven events from March to December 2011).

(2) In some areas where there had been no events before the Tohoku EQ, two repeating earthquake sequences appeared: M3.2-3.9 events (Group B) to the northwest of Group A and M2.2-4.4 events (Group C) to the northeast of the Group A. The centroids of the events in the Groups A-C were estimated to be located within 1 km.

(3) Magnitudes of the events in each group tended to become smaller as time passed. The Group-C events disappeared after the M2.2 event in January 1, 2012.

The phenomena similar to (1) were previously reported by Chen et al. (2010) and Uchida et al. (2015). These suggest that conditionally stable regions around the Group-A patch slipped seismically with the patch due to fast loading rate caused by afterslip of the Tohoku EQ. The phenomena in (2) can be interpreted as slip behavior changes in conditionally stable regions from aseismic to seismic due to the fast loading rate. The phenomena in (3) can be interpreted as that the rupture areas in the conditionally stable regions gradually shrunk over time as the loading rate decreased.

These results suggest that slip behavior changes that were probably dependent on the loading rate could cause not only changes in magnitudes but also emergence and disappearance of repeating earthquakes in some cases. These observations will be useful in the modeling of the plate boundary off Tohoku.

Acknowledgement: We used earthquake catalog and phase data produced by Japan Meteorological Agency. We also used waveform data from National Research Institute for Earth Science and Disaster Prevention, Hokkaido University and Hirosaki University.

Keywords: repeating earthquake, 2011 Tohoku earthquake, hypocenter relocation, conditionally stable region, afterslip

Japan Geoscience Union Meeting 2015
(May 24th - 28th at Makuhari, Chiba, Japan)

SSS30-23 Room:A05 Time:May 25 17:00-17:15

Early rupture process of the 14 March 2014 Iyo-Nada intermidiate-depth earthquake

SAITO, Mamoru[1] ; KOMATSU, Masanao[2*] ; TAKENAKA, Hiroshi[2]

[1]Okayama University, [2]Okayama University

An intermediate-depth earthquake (M_{JMA} 6.2) occurred in Iyo-Nada on March 14, 2014. The focal depth is 78 km, and this event occurred in the Philippine Sea slab. In this study, we investigate the early rupture process of this earthquake for about 5 seconds after the initial break. Three characteristic P-wave phases, P1, P2 and P3 are identified on the observed waveform records. Later phases has larger amplitude among the three phases. We estimate the generated position and time using the relative arrival time from the initial P phase for each of the three phases. We use vertical component of velocity waveform records at 52 seismic stations from the networks of JMA, NIED, AIST and Kyushu University, which are located at less than 105 km of epicentral distance, and read the arrival times and the polarities of the three phases and the first P arrival. Comparing the polarities of each arrival phase to the focal mechanism solution and the CMT solution from JMA, P1 phase corresponds to the focal mechanism, while P2 and P3 phases correspond to the CMT solution. Therefore, P1 phase is an initial rupture phase, while P2 and P3 phases are main rupture phases. The rupture position and time for each phase are estimated by the method of Takenaka *et al.* (2006, EPS) and its extension. As results, we found that initial P and P1 phases occurred on the east-dipping fault plane of the focal mechanism solution, while P2 and P3 occurred on north-dipping fault plane of the CMT solution. The two fault planes are crossover. The rupture moved from the initial rupture fault plane to the main rupture one. Focusing on the rupture times of the three phases, P1 phase was emitted by an event on the initial rupture fault plane at 0.49 seconds after the origin time of this earthquake. P2 phase then was generated by an event on the main rupture fault plane at 1.82 seconds after the origin time. P3 phase was emitted by a larger event at 3.3 seconds after the origin time.

Keywords: Rupture process, Initial rupture, Main rupture, Iyo-Nada

Japan Geoscience Union Meeting 2015
(May 24th - 28th at Makuhari, Chiba, Japan)

SSS30-24 Room:A05 Time:May 25 17:15-17:30

Evolution of rupture style with total fault displacement: insight from meter-scale direct shear experiments

XU, Shiqing[1*] ; FUKUYAMA, Eiichi[1] ; YAMASHITA, Futoshi[1] ; MIZOGUCHI, Kazuo[2] ; TAKIZAWA, Shigeru[3] ; KAWAKATA, Hironori[4]

[1]Nat'l Res. Inst. Earth Sci. Disas. Prev., [2]Centr. Res. Inst. Elect. Pow. Ind., [3]University of Tsukuba, [4]Ritsumeikan University

We report results with Indian metagabbro (Vs=3.62 km/s) that are obtained from a series of meter-scale direct shear experiments conducted at NIED. We focus on strain gage array data of stick-slip events loaded with 0.01 mm/s and under 6.7 MPa normal stress, and find the following: (1) During the early stage when the contact surface is relatively intact with less than 10 mm total displacement, ruptures mainly behave as slow-slip events (10 to 100 m/s). (2) With the accumulation of total fault displacement (up to several tens of mm), grooves indicative of strongly coupled local patches (i.e. asperities) are generated along the sliding surface, which are primarily elongated along the loading direction and are accompanied by notable gouge formation. The rest part of the surface continues being polished, indicated by a contrast in light reflectivity with respect to the initial level. At this stage, rupture speeds start to increase but are still well below the shear wave speed (˜1/4Vs). (3) After long enough total fault displacement (>500 mm), grooves and gouges of a sufficient amount are generated. The corresponding ruptures show, following a slow nucleation phase, fast propagation with speed comparable to the shear wave speed. Detailed strain data analysis shows that the above rupture style evolution is associated with an increasing efficiency in releasing the stored strain energy along the synthetic fault, which may have been facilitated by powder lubrication (Reches and Lockner, 2010) only after the formation of certain amount of gouges. Our study highlights the role of (evolving) fault surface properties in controlling propagation style of dynamic ruptures. It also calls for the need to conduct large-scale friction experiments over long displacement to better approximate natural fault conditions.

Keywords: Friction experiments, Dynamic rupture propagation, Fault lubrication

Japan Geoscience Union Meeting 2015
(May 24th - 28th at Makuhari, Chiba, Japan)

SSS30-25 Room:A05 Time:May 25 17:30-17:45

Cohesive Zone Length of Gabbro at Supershear Rupture Velocity (2)

FUKUYAMA, Eiichi[1*] ; XU, Shiqing[1] ; MIZOGUCHI, Kazuo[2] ; YAMASHITA, Futoshi[1]

[1]Nat'l Res. Inst. Earth Sci. Disas. Prev. (NIED), [2]Cntr. Res. Inst. Elect. Pow. Ind. (CRIEPI)

We investigated the shear strain field ahead of a supershear rupture. The strain array data along the sliding fault interfaces was obtained during large-scale biaxial friction experiments conducted at NIED in March 2013. These friction experiments were done using a pair of meter-scale metagabbro rock specimens whose simulated fault area was 1.5m x 0.1m. 2.6MPa normal stress was applied with loading velocity of 0.1mm/s. Along the fault edge parallel to the slip direction, 32 2-component semi-conductor strain gauges were installed at an interval of 50mm and 10mm off the fault. The data are conditioned by high frequency strain amplifiers (<0.5MHz) and continuously recorded at an interval of 1MHz with 16-bit resolution. Many stick-slip events were observed in this experiment. We chose unilateral rupture events in which foreshocks did not precede ahead of the main rupture and that propagated with supershear rupture velocity. One of the reasons for this selection was to improve the quality of observed data because the strain field ahead of the supershear rupture was not contaminated by elastic waves. Focusing on the rupture front, stress concentration was observed and sharp stress drop occurred immediately inside the rupture. We converted the temporal variation of strain to spatial variation of strain and picked up the peak strain and zero-crossing strain locations to measure the cohesive zone length. By compiling the stick-slip events, the cohesive zone length is 10 ˜20 mm. We could not see any systematic variation at the location but the cohesive zone length scattered between the events. We found that the cohesive zone length decreases with the total amount of slip as well as the rupture velocity increases, especially larger than root 2 times the shear wave velocity. This feature is more or less consistent with the theoretical prediction of Broberg (1999).

Keywords: cohesive zone, earthquake rupture, friction experiment, supershear rupture

Japan Geoscience Union Meeting 2015
(May 24th - 28th at Makuhari, Chiba, Japan)

SSS30-26 Room:A05 Time:May 25 17:45-18:00

Effects of plasticity on stick-slip behaviors of halite gouge

HIRAUCHI, Ken-ichi[1*] ; YOSHIDA, Yoshiaki[1] ; YABE, Yasuo[2] ; MUTO, Jun[3]

[1]Department of Geosciences, Graduate School of Science, Shizuoka University, [2]Graduate School of Science, Tohoku University, [3]Department of Earth Science, Graduate School of Science, Tohoku University

Non-volcanic tremors in subduction zones and San Andreas are known to be located near the bottom edge of the seismogenic zone. Assuming that the occurrence of ordinary earthquakes is inhibited by the onset of crystal plasticity in rock-forming minerals (e.g., quartz and feldspar), this implies that tremor activity occurs at the depth of a transition between brittle and ductile deformation. Previous studies of rock friction (Shimamoto, 1986, *Science*; Noda and Shimamoto, 2010, *GRL*) have already indicated that halite is a good candidate to explore the effects of plasticity on frictional behavior in laboratory, because with increasing normal stress (σ_n), the deformation mechanism of halite changes from frictional sliding to dislocation creep even at room temperature. However, it remains unclear how plasticity affects stick-slip behaviors of halite, including stress-drop magnitude, recurrence interval, frictional velocity dependence (a-b), and rupture propagation process.

To explore the effects of plasticity on stick-slip behavior, we conducted friction experiments on halite gouges at room temperature, constant normal stresses of 10 to 120 MPa, and sliding velocities of 1 or 10 μm/s, using a large biaxial testing machine installed at Tohoku University. Seven strain gauges were mounted on a forcing block at 23 mm intervals along the fault. For each experiment, we recorded more than 50 stick-slip events in total. At sliding velocity of 1 μm/s, the magnitude of stress drop increased from 1 MPa at σ_n = 10 MPa to 3 MPa at σ_n = 30 MPa, while decreasing to 0.5 MPa at σ_n = 120 MPa. The stick-slip recurrence interval at the same sliding velocity decreased from 20 s at σ_n = 10 MPa to 4 s at σ_n = 120 MPa. (a-b) values decreased from -0.005 at σ_n = 10 MPa to -0.025 at σ_n = 40 MPa, while remarkably increasing to 0.015 at σ_n = 120 MPa. Critical length (L_c) at which unstable, fast rupture propagation ($>$10% V_s) starts seems to increase with increasing σ_n.

Our experimental results indicate that the stick-slip behavior of halite fault gouges dramatically changes with increasing degree of plasticity, i.e., sharp, large stick-slip events in brittle regime evolve to smooth, small oscillations in semi-ductile (plastic) regime. Source characteristics of the small oscillations with sustained slow rupture may be linked to those of slow earthquakes such as non-volcanic tremors. It is well known that extremely low effective normal stress on the fault is the primary control on the occurrence of slow earthquakes. Furthermore, we suggest that the onset of plasticity in minerals, leading to an increase in (a-b), also facilitates the emergence of such slow transient creep events.

Keywords: friction experiments, halite, non-volcanic tremor, plasticity, rupture propagation, stick slip

Japan Geoscience Union Meeting 2015
(May 24th - 28th at Makuhari, Chiba, Japan)

SSS30-27 Room:A05 Time:May 26 09:00-09:15

Source Process of the 2014 ML5.5 Orkney earthquake, South Africa

OKUBO, Makoto[1*] ; CICHOWICZ, Artur[2] ; BIRCH, Denver[2] ; OGASAWARA, Hiroshi[3] ; MURAKAMI, Osamu[3] ; HORIUCHI, Shigeki[4]

[1]TRIES, ADEP, [2]Council for Geoscience, [3]Ritsumeikan Univ., [4]Home Seismometer Corp.

An earthquake occurred at 12:22:33 SAST (10:22:33 UT) on 5 August, with the epicenter near Orkney town near gold mines in the Klerksdorp district in the North West province of South Africa. The Council for Geoscience (CGS) in South Africa reported that the magnitude was M_L5.5. As a quick preliminary report, USGS estimated a left lateral fault mechanism and a focal depth of 5.0 km. CGS revised its depth to 4.7 km using the dense cluster network data. CGS also reported 84 aftershocks on 5 August and 31 aftershocks on 6 August, with magnitudes of 1.0 to 3.8 on the Richter scale. According to the CGS, this earthquake was the biggest recorded earthquake in the gold mining districts in South African history.

In this study, we analyzed the main shock waveforms and aftershock distribution to understand the rupture process of this earthquake. At the time of the 2014 Orkney earthquake, 17 strong motion surface stations were in operation and continuous acceleration seismograms were obtained with 24-bit and 200 Hz sampling. First, we picked P and S wave arrival times of the main shock and found two sets of phases in those seismograms. One belongs to a smaller event that occurred at a depth of 4.1 km (5.6 km below ground surface; BGS) with a magnitude less than 3. The other event started 0.3 seconds later with a larger magnitude slightly (1 km) north of the first one and at a depth of 4.2 km depth (5.7 km BGS). It seemed appears that the smaller initial rupture was leading led to a larger main rupture. According to the S wave velocity structure of in the Klerksdorp area, the S wave of the initial rupture can would have been able to reach to get to the hypocenter of the main rupture hypocenter, just in time. Thus, it seems that appears as though the initial rupture's S wave had initiated the main rupture.

Next, we applied hypoDD (Waldhauser & Ellsworth, 2000), the Double-Difference earthquake location algorithm, to P and S wave arrival times of the aftershocks, as well as to the initial and main ruptures of the main shock. We found spatial gaps in the deep parts of the aftershock distribution. These seem to correspond to the initial and main rupture hypocenters. We also found a horizontal seismic gap at a depth of 3.5 km BGS. Shallow events located above this seismic gap may have been caused by the M_L5.5 coseismic stress change and the existence of high mining rock stress. These might not be aftershocks since the gold mine leaf reaches up to a depth of 3.5 km.

According to Matsuda's law (Matsuda, 1975), the extent of a M_L5.5 earthquake fault can be 2-3 km (maximum for unidirectional rupture), main rupture could reach 2.5 km BGS. However, the existence of the horizontal seismicity gap and rupture extension at the same depth may imply that the main rupture did not reach 3.5 km BGS.

Keywords: SATREPS, initial rupture, Klerksdorp, double difference hypocenter location

Japan Geoscience Union Meeting 2015
(May 24th - 28th at Makuhari, Chiba, Japan)

SSS30-28 Room:A05 Time:May 26 09:15-09:30

Mitigation of the rockburst risk in deep South African gold mines

DURRHEIM, Raymond[1*] ; MILEV, Alexander[2] ; KGARUME, Thabang[2] ; BRINK, Van zyl[2] ; CICHOWICZ, Artur[3] ; OGASAWARA, Hiroshi[4]

[1]CSIR, South Africa, [2]University of the Witwatersrand, South Africa, [3]Council for Geoscience, South Africa, [4]Ritsumeikan University, Japan, [5]SATREPS

Earthquakes pose a significant risk to workers in deep and overstressed mines, such as South African gold mines. A 5-year collaborative project entitled OBSERVATIONAL STUDIES IN SOUTH AFRICAN MINES TO MITIGATE SEISMIC RISKS was launched in August 2010 to gain knowledge, develop and transfer technology, and build capacity. It was funded by the JST-JICA Science and Technology Research Partnership for Sustainable Development (SATREPS).

Rockbursts are seismic events that cause damage to underground workings. Strategies to mitigate the risk posed by rockbursts can be divided into three categories: prevention, protection and prediction. In this paper we will discuss the contribution made by the SATREPS project to these strategies.

Research sites were established at three deep gold mines: Cooke #4 Shaft, Hlanganani and Moab Khotsong. Boreholes were drilled to locate faults accurately that were considered capable of producing mining-induced seismic events. A variety of sensors were installed to monitor the quasi-static deformation of the rock mass, the accumulation of strain, tilt changes during the seismic event and post seismic creep phase, and changes in dynamic stress produced by the propagation of the rupture front. The Council for Geoscience (CGS) deployed 10 surface seismic stations in the Far West Rand district where the Cooke #4 and Hlanganani mines are situated. The CGS also manages a 25-station network established in the Klerksdorp district where the Moab-Khotsong mine is situated. SATREPS also provided a Kinemetrics Antelope Seismic Processing System to handle the large volume of data being acquired by the networks and the Horiuchi algorithm to automatically pick P- and S-arrival time and locate events.

By prevention, we mean a reduction in the occurrence of damaging seismic events. This is achieved by optimizing the design and sequence of extraction. Rock properties and the stress field are essential inputs. The SATREPS project has made a significant contribution to the mine design capability by adapting and transferring of the Compact Conical Borehole Overcoring (CCBO) stress measurement technique. Stress measurements, together with observations of borehole breakouts and discing of borehole core and seismic source parameters, are used to calibrate numerical models of mining layouts and sequences.

By protection, we mean the creation of rockburst-resistant excavations. As part of the SATREPS project we have studied the state of the rockwall in stopes near the research sites, measured the response of the rockmass to mining, and studied the performance of support elements and systems. In a complementary project, CSIR is developing various technologies to enable the stability of the hangingwall to be mapped prior to the entry of miners. These include robust closure and ground motion meters, thermal and acoustic mapping of hangingwall stability, and a robotic platform to carry these devices.

By prediction, we mean the reliable and timely forecasting of rockbursts so that mine workers may take refuge. We have used the unprecedented volume of high quality data gathered at the SATREPS sites to search for forerunners of seismic events. While we have gained new insights into the development of mining-induced fractures and the nucleation of seismic events, and studied variations in seismic parameters such as the b-value, we have not yet found a reliable precursory signal that can be used to raise an alarm.

Other lasting benefits of the SATREPS project include: (1) the enhancement of the National Seismograph Network, and (2) opportunities for several young South African researchers to visit Japanese institutes and gain experience in high-level research. The SATREPS project has been an extremely valuable contribution to researchers and practitioners working in deep South African mines, and we are grateful for the contributions of many dedicated Japanese scientists and the support of the Japanese government through JST and JICA.

Keywords: Mining induced seismicity, rockbursts, deep mines, South Africa, mitigation

Japan Geoscience Union Meeting 2015
(May 24th - 28th at Makuhari, Chiba, Japan)

SSS30-29 Room:A05 Time:May 26 09:30-09:45

Routine Estimation of Source Parameters of Mining-Related Earthquakes

CICHOWICZ, Artur[1*] ; BIRCH, Denver[1] ; MIYAKE, Hiroe[2] ; HORIUCHI, Shigeki[3] ; OGASAWARA, Hiroshi[4] ; DURRHEIM, Raymond[5] ; CGS, Technical team[6] ; THE SATREPS, Research group.[7]

[1]Council for Geoscience, South Africa / SATREPS, [2]The University of Tokyo, Japan / SATREPS, [3]Home Seismometer Corporation, Japan, [4]Ritsumeikan University, Japan / SATREPS, [5]University of the Witwatersrand and CSIR, South Africa / SATREPS, [6]Council for Geoscience, South Africa, [7]SATREPS (JST-JICA Science and Technology Research Partnership for Sustainable Development)

Mining in the Witwatersrand region of South Africa has led to induced seismicity. Seismicity is concentrated in several clusters associated with current mining production and flooding in abandoned mining voids. Starting in 2010, a surface network consisting of over 60 strong ground motion seismograph stations was installed in three clusters. Automatic earthquake location software from Home Seismometer Corp. based on an automatic location algorithm developed by Dr. Horiuchi was used to locate the large number of aftershocks quickly and accurately. Software for the estimation of seismic source spectral parameters was developed. The software is robust and most of the processing is performed automatically in a batch mode. A catalogue of a few thousand earthquakes was created and the spectral parameters of the events were estimated. Systematic shifts in the range of the spectral parameters for the three clusters were observed. Fluid-induced seismic events have a much smaller static stress drop (0.02- 5MPa) compared to areas where active mining is present (0.1-40MPa). The scalar seismic moment varied from 10^{10} to 10^{14} Nm for the fluid-induced seismicity cluster and for active mining it varied from 10^{10} to 10^{15} Nm. The relationships between static stress drop and scalar seismic moment undoubtedly show that the stress drop increases with seismic moment. Nevertheless, the scattering of the static or apparent stress drop around a fixed seismic moment spans roughly 1.5 -2.0 orders of magnitude.

An unexpectedly large earthquake of magnitude M_L 5.5 (M_w 5.3) was recorded in a district where active mining is currently taking place. Spectral analysis was performed in the frequency range 0.2 - 80Hz. An assumed quality factor of Q=400 was used. This value is used by underground mining networks. Kappa was set to 0.005. Analyzed waveforms were restricted to those recorded at small distances (2-20km) to reduce the effect of a possible error associated with the correction for path effects. The distribution of aftershocks located in the first 24 hours indicates the length of rupture zone to be roughly 6 km; however, spectral analysis of the entire S-wave group shows a maximum source size of approximately 2 km (S-wave corner frequency 1-1.3Hz). Visual inspection of the waveform clearly shows three sub-events. The first one is small followed by two stronger sub-events with similar pulse durations. The two strong sub-events occur about 0.5 sec apart. Analysis of the main event and aftershocks showed that the main event had a static stress drop of 35-45MPa, while the biggest aftershocks recorded in the first 10 days have static stress drops of 25-30MPa, and the largest aftershocks recorded in the next 10 days have static stress drops in the range 7-10MPa. The aftershocks with the largest static stress drops are distributed across the entire 6 km rupture zone. The relationship between stress drop and scalar seismic moment for all the aftershocks showed that the stress drop increases with seismic moment. The static stress drop varies in the range from 0.1 to 40MPa and scalar seismic moment varies from 10^{10} to 10^{14} Nm. The main event appears as a strong outlier with large scalar seismic moments of 2.6x10^{16} - 10^{17}Nm on the three components.

Keywords: spectral source parameters, induced seismicity, routine processing, static stress drop